

Exponential-type Constitutive Equation in Order to Use in Modeling the Warm Deformation of a Eutectoid Steel

H. Rastegari ¹, M. Rakhshkhorshid ^{2*}

Department of Mechanical and Materials Engineering, Birjand University of Technology, P.O.Box: 97175-569, Birjand, Iran

Abstract

The main contribution of the present work is to investigate the capability of exponential-type constitutive equation to model the warm deformation flow curves of a eutectoid steel in the temperature range of 620-770 °C and at the strain rates in the range of 0.01-10 s⁻¹ conducted on a Gleeble-1500 thermomechanical simulator. Warm deformation in this temperature range facilitates the occurrence of dynamic spheroidization of cementite lamellae as a softening process as well as some instabilities and microstructural defects. The prediction capability of the examined model was assessed using the average absolute relative error (AARE) criterion. The obtained AARE with the value of 7.39% for warm deformation modeling of the tested steel showed the acceptable performance of the examined model.

Keywords: Warm deformation; Flow stress; Exponential-type constitutive equation; Eutectoid steel; Dynamic spheroidization.

1. Introduction

Eutectoid steels are extensively used as pre-stressed concrete wires, rail steels and cold head bolts ¹⁻³. A new idea to improve the ductility of these steels is to convert the lamellar structure of fully pearlitic microstructure to a fine dispersion of nano or ultrafine spheroidized cementite particles in ferritic matrix through warm deformation near the eutectoid transformation temperature. The main softening process during warm deformation is dynamic spheroidization which occurs in specific applied strain, deformation temperature and strain rate ^{4,5}. Indeed, these deformation parameters must be carefully controlled. In this regard, mathematical simulation of warm deformation process of the eutectoid steels is a suitable way to control the deformation parameters and consequently, for successful production of the steel.

Modeling the mechanical response of the material to the external loading is the first step in mathematical

simulation which is conducted using the constitutive equations. Till now, many different constitutive equations have been developed and applied to model the materials behavior at elevated temperatures. The exponential-type constitutive equation is one of these equations that has ever been developed and used to model the hot deformation flow curves of different materials. As reported elsewhere, this equation is suitable for relatively low temperatures and relatively high strain rates ⁶⁻⁸.

To the best of authors' knowledge, no significant data are available in the literature on the warm deformation modeling of eutectoid steels through the constitutive equations and the only related work in this scope is the research conducted by Rakhshkhorshid and Rastgari ⁹. Rakhshkhorshid and Rastgari used a neural network with feed forward topology and Bayesian regularization training algorithm to predict the warm deformation flow curves of a eutectoid steel. The main contribution of the present work was to model the warm working behavior of eutectoid steel using exponential-type constitutive equation during single-hit compression testing. Furthermore, the observed deformation mechanisms of the eutectoid steel during warm working were briefly discussed from the metallurgical aspects.

2. Experimental Procedure

The material used in this study was a 12 mm diameter hot-rolled eutectoid steel rod supplied by

* Corresponding author

Tell: +98 56 322 52114, Fax: +98 56 322 52114

Email: rakhshkhorshid@birjandut.ac.ir

Address: Department of Mechanical and Materials Engineering, Birjand University of Technology, P.O.Box: 97175-569, Birjand, Iran

1. Assistant Professor

2. Assistant Professor

Nippon Steel Corporation. Chemical composition (in wt. %) of the eutectoid steel is listed in Table 1. The initial microstructure consists of a fully pearlitic microstructure with true interlamellar spacing of about 290 nm. Cylindrical specimens of $\phi 8$ mm x 10 mm were machined from the steel rod. To minimize friction and barreling effect, a graphite foil and tantalum foil was employed as a lubricant between the tungsten carbide anvils and the specimen surface during compression testing. Single-hit warm compression tests were performed in a Gleeble 1500[®] thermomechanical simulator in the deformation temperature of 620, 670, 720 and 770 °C and constant true strain rates of 0.01, 0.1, 1 and 10 s⁻¹ to a true strain of 0.5. For metallographic examination, deformed specimens were sectioned at mid-plane parallel to the compression axis. Microstructures were characterized in the central location of each specimen using scanning electron microscopy (Philips XL30).

Table 1. Chemical composition of the eutectoid steel (wt. %).

C	Si	Mn	P	S
0.82	0.18	0.66	0.012	0.005

3. Result and Discussion

3.1. Flow behavior and microstructure

Flow stress correction of true stress- true strain curves was carried out based on the Gleeble application note, numbered APN002¹⁰⁾. In addition, the flow curve was smoothed by fitting a seventh to ninth-order polynomial regarding to the LOESS method (a non-parametric regression method: locally weighted scatterplot smoothing (LOESS); sampling proportion: 0.1). Smoothed true stress-strain curves obtained for different temperatures and strain rates are summarized in Fig. 1. As can be seen, the flow behavior of the eutectoid steel was affected by deformation temperature and the strain rate. The flow stress tends to increase with decreasing the temperature and increasing the strain rate. In addition, the higher strain rate at a given temperature leads to an increase in peak stress. For deformation temperatures less than or equal to 720 °C, the flow stress beyond the peak stress decreases continuously with strain. Moreover, the extent of flow softening decreased with increasing temperature and decreasing the strain rate, irrespective of the strain rate. It is obvious that the onset of dynamic spheroidization of cementite lamella during warm compression, due to the softening effect, identified by a single peak stress at relatively low strains followed by a gradual fall, which is similar to what can be observed in typical instances of dynamic recrystallization (DRX) phenomenon⁴⁾. However, at 770 °C, at the early stage of deformation, work hardening dominates flow softening, and a rapid increase of flow stress appears.

As the strain increases, hardening and softening rates reach to equal values and the curves exhibit a steady-state behavior. The flow stress at higher strain rates approaches almost flat behavior, particularly at higher strains.

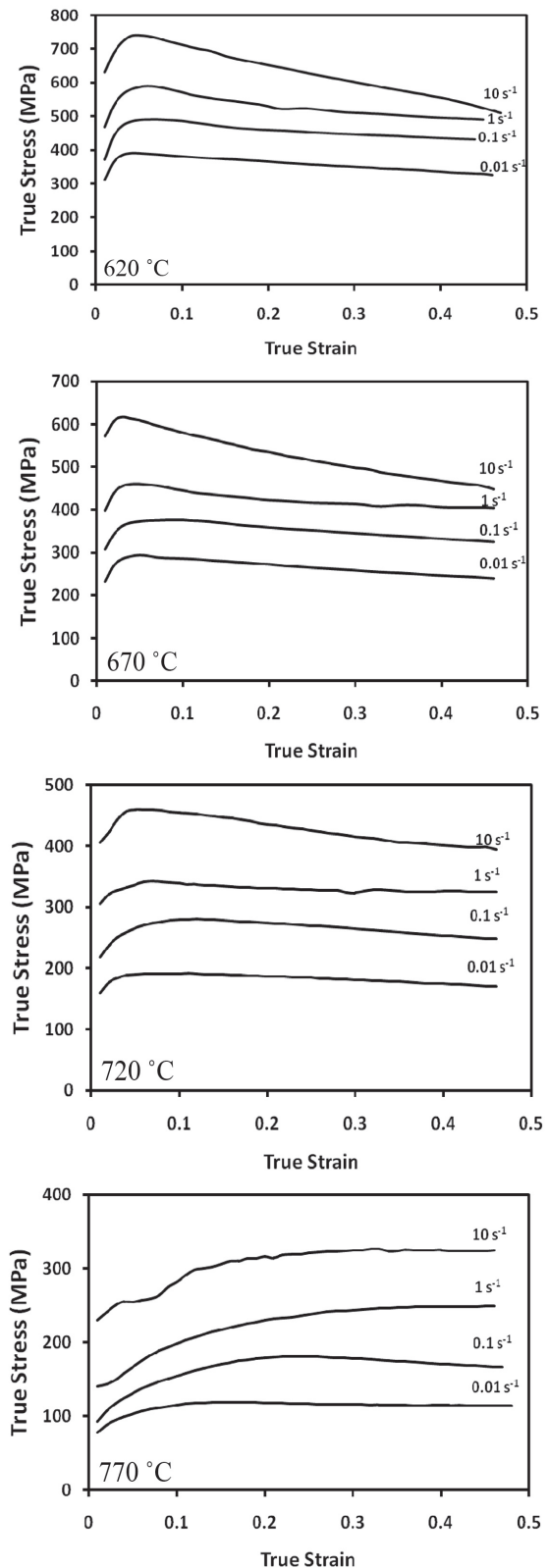


Fig. 1. Experimental flow curves of eutectoid steel at different warm deformation conditions.

An example of nearly complete DSX microstructure that was expected from the shape of flow curve is exhibited in Fig. 2a, which shows the microstructure obtained at the temperature of 720 °C and the strain rate of 0.01 s⁻¹. However, by decreasing the deformation temperature and increasing the strain rate, some deformation defects have been observed, besides the occurrence of DSX. Fig. 2b shows lamella cracking of the lamella under compressive strain. A detailed account of the deformation mechanisms operating during warm working of eutectoid steel has been elaborated elsewhere ⁴⁾.

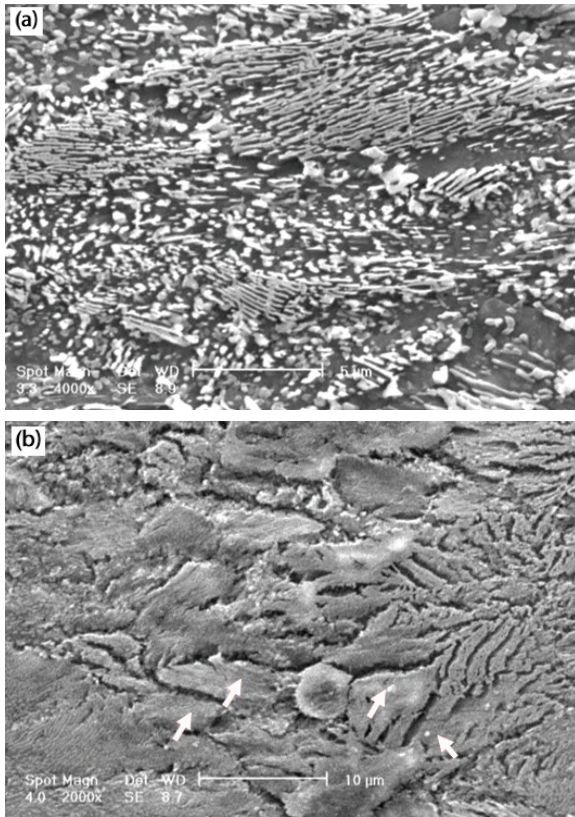


Fig. 2. Microstructure of samples deformed at (a) dynamic spheroidization at 720 °C / 0.01 s⁻¹ and (b) lamella cracking at 720 °C / 10 s⁻¹.

3. 2. Exponential-type constitutive modelling

As the flow curves of the metallic materials are affected by the temperature and the strain rate, it is a common practice to apply the equations in which the Zener–Hollomon parameter (Z) is considered a function of stress to describe the flow curves of different materials ^{11, 12)}:

$$Z = \dot{\epsilon} \exp\left(\frac{Q}{RT}\right) = f(\sigma) \quad (\text{Eq.1})$$

where Q is the activation energy (KJ/mol), R is the universal gas constant and T is the absolute deformation temperature. Substituting the exponential

law as an alternative of $f(\sigma)$:

$$Z = \dot{\epsilon} \exp\left(\frac{Q}{RT}\right) = A'' \exp(\beta\sigma) \quad (\text{Eq.2})$$

where A'' and β are material constants. The equation above, could be rewritten for a characteristic stress (i.e. for the peak stress) or a stress corresponding to a certain strain (for example the stress corresponding to the strain of 0.3) ^{13, 14)}. Taking natural logarithm from Eq. (2) yields:

$$\ln \dot{\epsilon} + \frac{Q}{R} \left(\frac{1}{T}\right) = \ln A'' + \beta\sigma \quad (\text{Eq. 3})$$

Also, taking the partial differentiation from the equation above (Eq. (3)) gives:

$$\partial \ln \dot{\epsilon} + \frac{Q}{R} \partial \left(\frac{1}{T}\right) = \beta \partial \sigma \quad (\text{Eq. 4})$$

According to Eq. (4), for deriving the Exponential-type constitutive equation with strain dependent constants, the following procedure should be performed to find the values of material constants of β and $\ln A''$ together with the values of activation energy (Q) for the stresses corresponding to different strains in a predefined interval and step size. Then, Polynomial curve fitting could be applied to express these material constants as polynomial functions of strain ¹³⁻¹⁵⁾.

1) The value of β should be obtained from the $\ln \dot{\epsilon}$ - σ plot (as a result of writing the Eq. (4) for temperature constant conditions). The average slope obtained from this plot is considered as the value of β . The $\ln \dot{\epsilon}$ - σ diagrams plotted for the stresses corresponding to the strains of 0.3 to determine the average value of β are presented in Fig. 3.

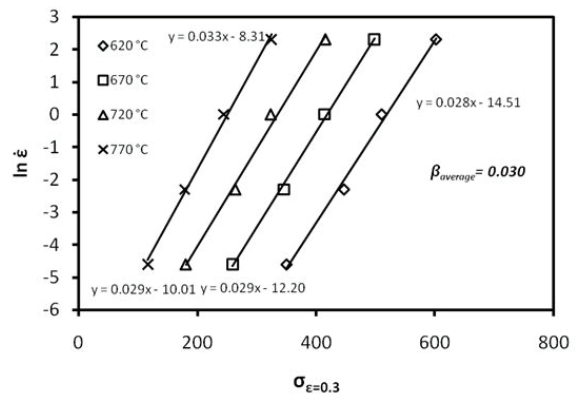


Fig. 3. The $\ln \dot{\epsilon}$ - σ diagrams plotted for the stresses corresponding to the strains of 0.3 to determine the average value of β .

2) The value of Q should be obtained from the σ -1/T plot (as a result of writing the Eq. (4) for $\dot{\epsilon}$

constant conditions). The σ - $1/T$ diagrams plotted for the stresses corresponding to the strains of 0.3 to determine the average value of Q are presented in Fig. 4. The average slope obtained from this plot should be multiplied by $R^* \beta$ factor to obtain the value of Q (from writing the Eq. (4) for $\dot{\epsilon}$ constant conditions).

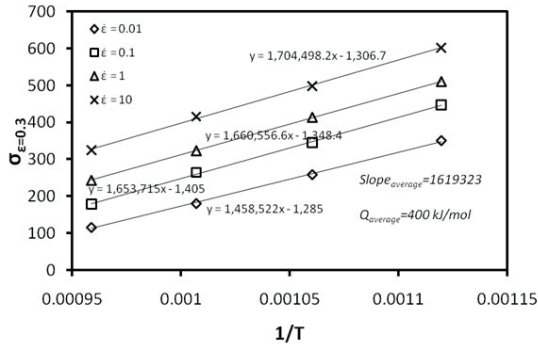


Fig. 4. The σ - $1/T$ diagrams plotted for the stresses corresponding to the strains of 0.3 to determine the average value of Q .

3) Rewriting the Eq. (3) for the tested deformation conditions (with different temperatures and strain rates) and substituting the obtained values of β and Q , an optimization procedure should be used to find the proper value of $\ln A''$. Here, the value of $\ln A''$ using a Newtonian optimization method, has been calculated equals to 38.59.

In a way similar to what conducted for the stresses corresponding to the strain of 0.3, the stages 1 to 3 were repeated to find the values of β , Q and $\ln A''$ at stresses corresponding to different strains in the range of 0.05 to 0.45 with the step size of 0.05. The overall results are presented in Fig. 5.

As depicted in this figure, the regression analysis was used to express the obtained constants as polynomial functions of strain. The results are summarized as in the bellow:

$$\beta = -0.038 \epsilon + 0.035 \epsilon^2 + 0.002 \epsilon + 0.026 \quad (\text{Eq. 5})$$

$$Q = -2,679,232.517 \epsilon^3 + 3,102,649.148 \epsilon^2 - 1,279,709.223 \epsilon + 592,420.562 \quad (\text{Eq. 6})$$

$$\ln A'' = -338.040 \epsilon^3 + 390.258 \epsilon^2 - 161.006 \epsilon + 62.757 \quad (\text{Eq. 7})$$

These strain dependent materials constants were substituted in the following equation (obtained from the Eq. (3)) to model the flow stress of tested steel:

$$\sigma = \left(\ln \dot{\epsilon} + \frac{Q}{RT} - \ln A'' \right) \beta \quad (\text{Eq. 8})$$

A comparison between the experimental and modeled flow curves (using the exponential-type constitutive equation with strain dependent constants) at different warm deformation conditions is presented

in Fig. 6.

3. 3. Evaluating the performance of the examined constitutive equation

In this paper, the average absolute relative error (AARE) was used to evaluate the modeling performance of examined constitutive equation:

$$\text{AARE} (\%) = \frac{1}{N} \sum_{i=1}^N \left| \frac{e_i - y_i}{e_i} \right| \times 100 \quad (\text{Eq. 9})$$

where e_i is the experimental output, y_i is the model output and N is the number of compared data. Using the exponential-type constitutive equation with strain dependent constants, the AARE value of 7.39 was obtained to model the flow curves of tested steel (Fig. 1). This, together in comparison to the experimental and modeled flow curves (Fig. 6) shows the acceptable performance of the examined equation.

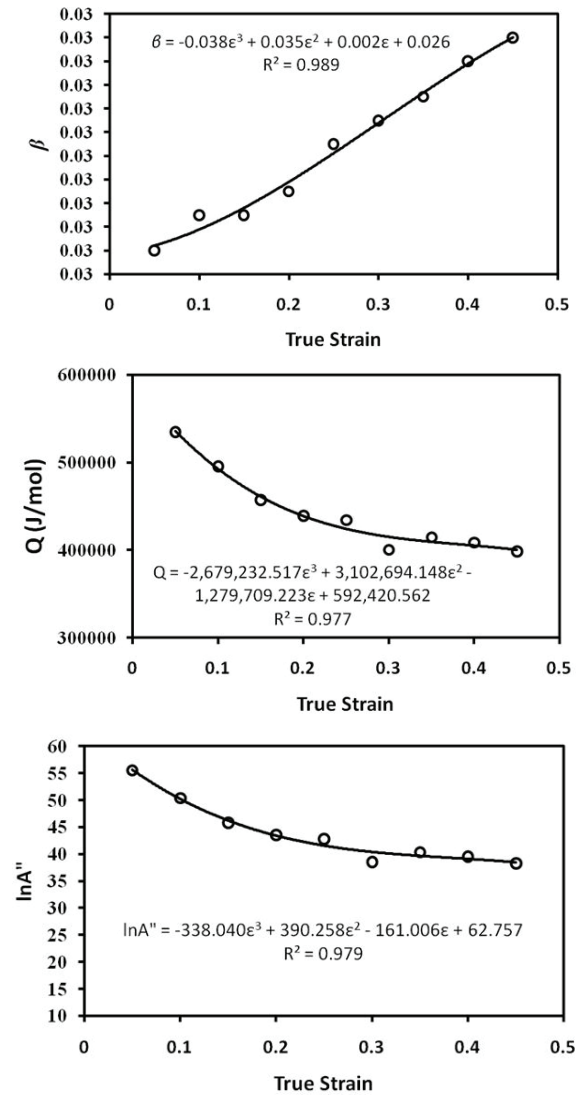


Fig. 5. Warm deformation constants of exponential-type constitutive equation as the function of true strain.

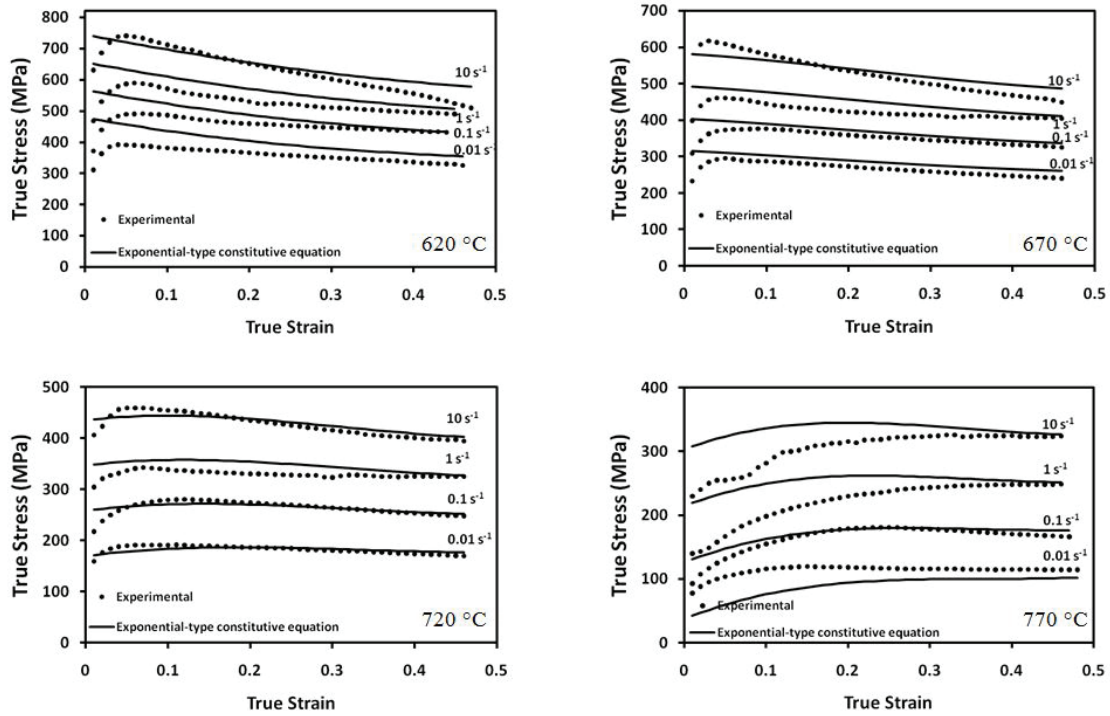


Fig. 6. The comparison between the experimental and modeled flow curves (using the exponential-type constitutive equation with strain dependent constants) at different tested warm deformation conditions.

It is worth mentioning that the deviation of experimental data and predicted flow curves seems to be higher at the temperature of 770 °C compared to the other deformation temperatures. Indeed, it can be due to the formation of austenite phase during the warm working. Based on the eutectoid transformation temperature of 720 °C, warm deformation in the temperature of 770 °C can be resulted in the formation of austenite phase, especially at the strain rate of 0.01 s⁻¹. Therefore, the situation becomes some complicated. On the other hand, transformation temperature of austenite to ferrite+cementite may be affected by warm deformation and it increases the transformation temperature. Hence, ferrite+cementite may be formed during warm working at the temperature of 770 °C.

4. Conclusions

In this research, the warm deformation flow stress of eutectoid steel was described through the exponential-type constitutive equation. The following conclusions can be drawn from this study:

- Using the exponential-type constitutive equation with strain dependent constants, the warm deformation flow stress of eutectoid steel can be described through the following equation:

$$\sigma = \left(\ln \dot{\epsilon} + \frac{Q}{RT} - \ln A'' \right) \beta$$

While the strain dependent constants of this equation were calculated as:

$$\beta = -0.038 \epsilon + 0.035 \epsilon^2 + 0.002 \epsilon + 0.026$$

$$Q = -2,679,232.517 \epsilon^3 + 3,102,649.148 \epsilon^2 - 1,279,709.223 \epsilon + 592,420.562$$

$$\ln A'' = -338.040 \epsilon^3 + 390.258 \epsilon^2 - 161.006 \epsilon + 62.757$$

- The average value of absolute relative error (AARE) criterion for the exponential-type constitutive equation was achieved as 7.39% that shows the acceptable performance of this constitutive equation in warm deformation modeling of eutectoid steel in the two phase field region (alpha+cementite).

References

- [1] C.W. Garrett: The Production of High Carbon Steel Wire, Rod and Wire Production Practice, The American institute of mining and metallurgical engineering, (1990).
- [2] G. Krauss: Steels; Processing, Structure, and Performance, ASM International, (2005).
- [3] T. Tarui, T. Takahashi, H. Tashiro, S. Nishida: Metallurgical Design of Ultra High Strength Steel Wires for Bridge Cable and Tire Cord, TMS, Warrendale, (1996).
- [4] H. Rastegari, A. Kermanpur, A. Najafizadeh, D. Porter, M. Somani: J. Alloys. Compd., 626(2015), 136.
- [5] T. Wu, M. Wang, Y. Gao, X. Li, Y. Zhao, Q. Zou: J. Iron. Steel. Res. Int., 19(2012), 60.

- [6] F. A. Slooff, J. Zhou, J. Duszczuk, and L. Katgerman: *Scripta Mater.*, 57(2007), 759.
- [7] H. Mirzadeh: *Mech. Mater.*, 85 (2015), 66.
- [8] H. Mirzadeh: *Metall. Mater. Trans. A.*, 46(2015), 4027.
- [9] M. Rakhshkhorshid, H. Rastegari: *Inter. J. ISSI*, 13(2016), 15.
- [10] Dynamic Systems Inc., Gleeble@ System Application Note APN002, (2001), 1-8.
- [11] H. Mirzadeh, J.M., Cabrera, J.M. Prado, A. Najafizadeh: *Metall. Mater. Trans A.*, 43(2012), 108.
- [12] H. Mirzadeh, J.M. Cabrera, J.M. Prado, A. Najafizadeh: *Mater. Sci. Eng. A.*, 528(2011), 3876.
- [13] M. Rakhshkhorshid: *Int. J. Adv. Manuf. Technol.*, 77(2015), 203.
- [14] M. Shaban, B. Eghbali: *Mater. Sci. Eng. A.*, 527(2010), 4320.
- [15] Y.C. Lin, M.S. Chen, J. Zhang: *Comp. Mater. Sci.*, 424(2008), 470.